Supporting Information

SI Text

General Methods. All solvents were of reagent grade. Acetonitrile and THF were dried by passing through activated alumina. 2-Cyano-6-hydroxybenzothiazole was from APIN Chemicals Ltd. All commercially purchased chemicals were used as received. ^{1}H and ^{13}C NMR spectra were obtained from a Bruker AVB-400 NMR spectrometer at the College of Chemistry NMR facility at UC Berkeley. Signals were internally referenced to solvent residues. Low resolution mass spectral analyses were carried out using a LCMS (Agilent Technology 6130, Quadrupole LC/MS). High resolution mass spectral analyses (ESI-MS) were carried out at the College of Chemistry Mass Spectrometry Facility at UC Berkeley.

Synthesis of 1. To a solution of 2,6-bis(bromomethyl)pyridine (460 mg, 1.74 mmol) and 2-cyano-6-hydroxybenzothiazole (200 mg, 1.14 mmol) in THF (50 ml) was added Cs_2CO_3 (450 mg, 1.38 mmol). The mixture was heated at 50 °C overnight, cooled to room temperature and filtered. The filtrate was concentrated and purified by SiO_2 column (hexane/ethyl acetate = 6:4). The product was isolated as white solid. Yield = 349 mg, 89%. ^{1}H NMR (400 MHz, CD_3OD, 298 K) δ (ppm): 8.10 (d, J = 9.2 Hz, 1 H), 7.87 (t, J = 7.6 Hz, 1 H), 7.77 (d, J = 2.8 Hz, 1 H), 7.55 (d, J = 7.6 Hz, 1 H), 7.51 (d, J = 7.6 Hz, 1 H), 7.42 (dd, J = 9.2 Hz, 2.8 Hz, 1 H), 5.30 (s, 2 H), 4.63 (s, 2 H). ^{13}C NMR (100.6 MHz, CD_3OD, 298 K) δ (ppm): 160.6, 158.3, 157.6, 148.5, 139.9, 138.9, 135.5, 126.6, 124.3, 122.6, 120.2, 114.1, 106.1, 72.0, 33.7. ESI-MS(+ve) calcd. for $C_{15}H_{11}N_3OS^{79}Br$ $[M+H]^+$ *m/z*: 360.0; found: 360.0; calcd. for $C_{15}H_{11}N_3OS^{81}Br$ $[M+H]^+$ *m/z*: 362.0; found: 362.2.

Synthesis of 2. To a solution of **1** (266 mg, 0.74 mmol) in 30 ml MeCN was added a solution of di(2-picolyl)amine (180 mg, 0.90 mmol, 10 ml) in MeCN, followed by addition of KI (30 mg, 0.18 mmol) and K_2CO_3 (820 mg, 5.9 mmol). The mixture was stirred at room temperature overnight and filtered. The filtrate was concentrated and purified by basic alumina column (ethyl acetate). The product was isolated as pale yellow oil. Yield = 193 mg, 54%. ^{1}H NMR (400 MHz, CD_3OD, 298 K) δ (ppm): 8.42 (d, J = 4.8 Hz, 1 H), 8.02 (d, J = 9.2 Hz, 1 H), 7.80-7.74 (m, 3 H), 7.69 (d, J = 2.4 Hz, 1 H), 7.64 (d, J = 8.0 Hz, 2 H), 7.55 (d, J = 7.6 Hz, 1 H), 7.43 (d, J = 7.6 Hz, 1 H), 7.35 (dd, J = 9.2 Hz, 2.8 Hz, 1 H), 7.25 (t, J = 6.2 Hz, 2 H), 5.24 (s, 2 H), 3.86 (s, 2 H), 3.85 (s, 4 H). ^{13}C NMR (100.6 MHz, CD_3OD, 298 K) δ (ppm): 160.6, 160.1, 156.8, 149.5, 148.3, 139.1, 138.9, 138.6, 135.4, 126.6, 124.9, 123.9, 123.8, 121.6, 120.2, 114.1, 106.0, 72.1, 61.1, 61.0. HRMS (ESI) calcd. for $C_{27}H_{23}N_6OS$ $[M+H]^+$ *m/z* = 479.1654; found: 479.1645; calcd. for $C_{27}H_{22}N_6OSLi$ $[M+Li]^+$ *m/z* = 485.1736; found: 485.1725.

Synthesis of CCL-1. To a Schlenk tube charged with D-cysteine hydrochloride monohydrate (78 mg, 0.44 mmol) and K_2CO_3 (70 mg, 0.51 mmol) in N_2 was added degassed water (1 ml), followed by a degassed MeOH solution of **2** (193 mg, 0.40 mmol, 2 ml). The solution was stirred under N_2 for 30 min, and pH was adjusted to 7. The volume was reduced and the crude material was purified by preparative HPLC on a 30 x 250 mm, 10 micron Agilent Prep-C18 column (flow rate = 20 ml/min, H_2O/MeCN with 0.05% formic acid gradient: 0-5 min, 22% MeCN; 5-15 min, 22% → 40% MeCN; 15-40 min, 40% MeCN). The product was isolated as a formate salt. Yield = 108 mg, 41%. ^{1}H NMR (400 MHz, CD_3OD, 298 K) δ (ppm): 8.47 (d, J = 4.4 Hz, 2 H), 8.16 (br s, 2 H), 7.83-7.72 (m, 4 H), 7.55 (d, J = 8.0 Hz, 2 H), 7.47 (d, J = 2.4 Hz, 1 H), 7.41 (d, J = 8.0 Hz, 1 H), 7.38 (d, J = 7.6 Hz, 1 H), 7.31 (d, J = 6.0 Hz, 1 H), 7.29 (d, J = 5.2 Hz, 1 H), 7.14 (dd, J = 9.2 Hz, 2.6 Hz, 1 H), 5.31 (br, 1 H), 5.13 (s, 2 H), 4.05 (s, 4 H), 4.02 (s, 2 H), 3.71 (br d, J = 7.2 Hz, 2 H). ^{13}C NMR (100.6 MHz, CD_3OD, 298 K) δ (ppm): 166.8, 165.3, 160.0, 159.3, 158.0, 157.9, 157.2, 149.0, 139.6, 139.3, 138.9, 125.9, 125.2, 124.5, 124.0, 122.0, 118.5, 106.4, 80.5, 71.1, 60.6, 60.3, 36.2. HRMS (ESI) calcd. for $C_{30}H_{27}N_6O_3S_2$ $[M+H]^+$ *m/z* = 583.1586; found: 583.1581.

***In Vitro* Luminescence Assays.** Millipore water was used to prepare all aqueous solutions. Incubation of CCL-1 with different metal ions ($MgCl_2$, $CaCl_2$, $MnCl_2$, $FeCl_2$, $FeCl_3$, $CoCl_2$, $NiCl_2$, $Cu(MeCN)_4(PF_6)$, $CuCl_2$ and $ZnCl_2$) was performed in 50 mM Tris buffer at pH 7.4, with 5 mM GSH and 5 μM of CCL-1 (100x dilution of a 500 mM stock in DMSO). Similar experiments were performed with D-luciferin (100 nM, 100x dilution of a 10 μM stock in Dulbecco's phosphate-buffered saline, or DPBS) to determine any effects of the metal ion treatments on luciferase activity. At the end of the incubation, 100 μl of the solution was transferred to a well of a white, opaque 96-well plate (Corning). An equal volume (100 μl) of a solution of luciferase (100 μg/ml, Promega) in 50 mM Tris buffer at pH 7.4, with 10 mM Mg^{2+} ($MgCl_2$), 0.1 mM Zn^{2+} ($ZnCl_2$) and 2 mM ATP was added and mixed well. Bioluminescent signals were measured using a Molecular Devices SpectraMax M2 plate reader at 37°C for 1 h. To determine the stability of CCL-1, 5 μM of the probe was incubated with or without 100 μM $CuCl_2$ and 5 mM GSH as a reducing agent in DMEM containing 10% FBS at room temperature. At 0, 1, 3, 6, 9, 12, and 24 hours after

incubation, 40 μL of the CCL-1 solution was transferred to a well of a white, opaque half-area 96-well plate (Corning). Luciferase assays were performed as described above using equal volumes (40 μL) of the luciferase solution.

Cellular Assays. A Xenogen IVIS Spectrum instrument (Caliper Life Sciences) was used for bioluminescence imaging in all cellular experiments. LNCaP-luc and PC3M-luc cells were cultured in DMEM containing 10% FBS. Prior to assaying, cells were passaged and plated (4.5×10^4 for LNCaP-luc and 1.5×10^4 for PC3M-luc cells per well) in black 96-well plate with clear bottoms (Becton, Dickson and Company). The cells were then supplemented and incubated with $CuCl_2$ (DMEM with 10% FBS) at different concentrations for 24 h. The medium was removed and 100 μl of CCL-1 (25 μM or 50 μM in DMEM with 2.5% DMSO) was added. The plate was immediately imaged for 2 h. For chelation experiments, NS3' (200 μM final concentration in DMEM) was added before addition of CCL-1. For control experiments, cells treated under the same conditions were imaged with 1 μM D-luciferin.

Animals. FVB-luc$^+$ (FVB-Tg(CAG-luc,-GFP)L2G85Chco/J) mice were obtained from our in-house breeding colony. To generate mice expressing luciferase exclusively in the liver, we purchased mice bearing the Gt(ROSA)26Sor$^{tm1(Luc)Kael}$ allele and Tg(Alb-cre)21Mgn mice purchased from Jackson Laboratories (stocks 005125 and 003574, respectively) and crossed the two strains. Gray-fur mice were bred several times to generate white-fur litters. Mice were group-housed on a 12 12 light-dark cycle at 22 °C with free access to food and water. All animal studies were approved by and performed according to the guidelines of the Animal Care and Use Committee of the University of California, Berkeley. For diet studies, separately housed 8-week-old male mice were fed a high-fat diet (60% calories from fat, Research Diets D12492), a low-fat diet (10% calories from fat, Research Diets D12450J), or a regular (or normal) diet (18% calories from fat, Teklad 2018) for 8 weeks. Weight and food intake were measured weekly. Standard glucose tolerance tests were performed in mice fasted for 12 h at the end of special diet feeding. The animals were sacrificed at either 4 weeks or 8 weeks after the feeding and their organs harvested for ICP-MS and Western blot analysis.

General Animal Imaging Methods and Data Analysis. A Xenogen IVIS Spectrum instrument (Caliper Life Sciences) was used for bioluminescence imaging in all animal experiments, and image analysis was performed using the Living Image software. The total photon flux for each animal was determined by drawing a region of interest around the entire animal (in FVB-Luc$^+$ mice) or around the apparent liver (in L-Luc mice) and integrating the photon flux over the total imaging period. Mice were anesthetized prior to injection and during imaging via inhalation of isoflurane. Isoflurane was purchased from Phoenix Pharmaceuticals, Inc. DMSO was purchased from Sigma-Aldrich, and medical-grade oxygen was purchased from Praxair.

Imaging Copper with CCL-1. FVB-luc$^+$ and L-Luc mice were given intraperitoneal (i.p.) injections of the following sets of compounds and/or vehicles under anesthesia (isoflurane inhalation 2-3%). FVB-luc$^+$ mice were injected with CCL-1 (0.2 μmol in 25 μL DMSO, 25 μL DPBS) after i.p. injection of vehicle (50 μL DPBS), $CuCl_2$ (3 mg/kg in 50 μL DPBS)), ATN-224 (5mg/kg in 50 μL DPBS) or both $CuCl_2$ (3 mg/kg in 50 μL DPBS) and ATN-224 (5 mg/kg in 50 μL DPBS). Injection of $CuCl_2$ and ATN-224 were performed 2 h and 10 min prior to injection CCL-1, respectively. L-Luc mice were injected (i.p.) with CCL-1 (0.1 μmol in 25 μL DMSO) after i.p. injection of vehicle (50 μL DPBS), $CuCl_2$ (3 mg/kg in 50 μL DPBS) alone, both $CuCl_2$ (3 mg/kg in 50 μL DPBS) and ATN-224 (5 mg/kg in 50 μL DPBS), or ATN-224 (30 mg/kg in 50 μL DPBS) alone. Injections of $CuCl_2$ or ATN-224 alone were performed 2 h prior to injection of CCL-1. Mice injected with both $CuCl_2$ and ATN-224 were injected 2 h and 10 min prior to injection of CCL-1, respectively. Following injection of CCL-1, mice were transferred to a Xenogen IVIS Spectrum (Caliper Life Sciences) and imaged for 60 min under isoflurane anesthesia (2%). To determine the dose-dependent responses of CCL-1 administration and copper treatment, experiments were performed in FVB-luc$^+$ as described above with varying amounts of CCL-1 (25 nmol - 0.1 μmol in 25 μL DMSO, 25 μL DPBS; 0.4 μmol in 35 μL DMSO, 15 μL DPBS) and/or varying amounts of $CuCl_2$ (0.3, 0.6, 1.5, and 6 mg/kg in 50 μL DPBS).

To determine the metabolic stability and clearance of the probe, FVB-luc$^+$ were given i.p. injections of 0.2 μmol CCL-1 or D-luciferin (25 μL DMSO, 25 μL DPBS). Images were acquired at 5 and 20 min, as well as 1, 3, 6, 9, 12, and 24 hours post-injection. For each time point, mice were anesthetized under isoflurane (2%) for 3 min prior to imaging, then transferred to a Xenogen IVIS Spectrum (Caliper Life Sciences) for image acquisition.

Tissue Harvesting and Inductively Coupled Plasma Mass Spectrometry (ICP-MS). Mice were heavily anesthetized, euthanized by cervical dislocation, and slowly perfused with DPBS (10-25 mL). Following perfusion, tissues were harvested and immediately placed on dry ice in cryotubes and stored in -80 ºC until analyzed. For ICP-MS analysis, 20-100 mg portions of the harvested tissues were digested in concentrated nitric acid (100 mg/mL HNO_3, BDH Aristar Ultra) at 90 ºC for 2 h in 1.5 mL tubes (Sarstedt) with small holes poked in the caps. After

overnight incubation at room temperature, samples were diluted into 2% HNO_3 and doped with a gallium internal standard (Inorganic Ventures, 20 ppb final concentration). The copper content was determined by measuring ^{63}Cu using a Thermo Fisher iCAP-Qc ICP-MS in Kinetic Energy Discrimination (KED) mode with the He flow set to 4.426 mL/min. Measurements were normalized to a standard curve of known copper concentrations doped with 20 ppb Ga. The standard curve was diluted from CMS-5 (Inorganic Ventures).

Tissue Lysis and Western Blot Analysis. Frozen mouse livers were minced into 5-10 mg samples on dry ice and homogenized in ice-cold RIPA buffer (25 mM Tris•HCl pH 7.6, 150 mM NaCl, 1% NP-40, 1% sodium deoxycholate, 0.1% SDS) containing protease inhibitor cocktail (Roche) using a hand-held mechanical homogenizer. Homogenates were incubated on ice for 30 min and centrifuged at 12,000 × g for 20 min at 4 ºC. The supernatants (including the resulting upper lipid layers were transferred to new tubes and centrifuged) were transferred to new tubes and centrifuged at 12,000 × g for 10 min at 4 ºC. The soluble protein lysates were collected from underneath the upper lipid layer with a pipette and transferred to new tubes and were subsequently used for Western blotting.

Protein concentration was determined using a BCA Assay (Pierce) containing 2% SDS to minimize lipid interference. The protein lysates were denatured in NuPAGE lithium dodecyl sulfate sample buffer (Invitrogen) containing ß-mercaptoethanol as a reducing agent. The samples (20-40 μg) were resolved by SDS-PAGE using NuPAGE 4-12% Bis-Tris gels (Invitrogen) with MES SDS running buffer (Invitrogen). Proteins were transferred to a polyvinylidene difluoride membrane (BioRad, Munich, Germany) with the use of the Trans-Blot Turbo transfer system (BioRad, Munich, Germany)).

The membranes were blocked in 5% non-fat dry milk in TBST buffer (10 mM Tris, pH 7.5, 100 mM NaCl, 0.1% Tween-20) for 30 min at room temperature. After blocking, the membranes were incubated at 4 ºC overnight with primary antibodies diluted with TBST buffer containing 5% bovine serum albumin (BSA). The anti-CCS (sc-20141, Santa Cruz Biotechnology) and anti-ATP7A (HP8040, Hycult Biotech) antibodies were used at 1:500 dilution and the anti-ATP7B antibody (ab135571, Abcam) was used at 1:100 dilution. The anti-Ctr1 antibody was kindly provided by Dr. Dennis J. Thiele (Duke University; Nose Y, Kim BE, Thiele DJ. *Cell Metab*. 2006, 4, 235-244) and used at a 1:2000 dilution. The membranes were washed 3 times for 5 minutes in TBST and incubated for 1 hour at room temperature with horseradish peroxidase (HRP)-conjugated anti-rabbit IgG secondary antibody (sc-2004, Santa Cruz Biotechnology) at a 1:2000 dilution in TBST containing 5% BSA. The membranes were washed 5 times for 5 minutes in TBST, then visualized using enhanced chemiluminescence (Western Lighting Plus for visualizing CCS, ATP7B, and CTR1; Western Lighting Ultra for visualizing ATP7A; Perkin-Elmer) recorded on a BioRad GelDoc imaging station. ß-actin was probed to determine equal loading using anti-ß-actin (sc-69879, Santa Cruz Biotechnology) and AlexaFluor 647-conjugated anti-mouse IgG (A31571, Molecular Probes) antibodies at 1:5000 and 1:2500 dilutions, respectively, with visualization using fluorescence recorded on a BioRad GelDoc imaging station.

Supporting Figures

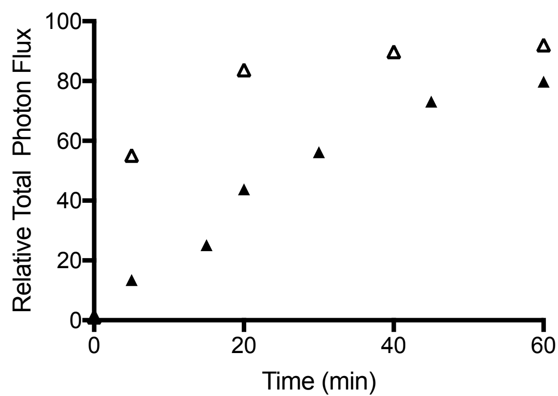

FIGURE S1. Relative bioluminescence response of CCL-1 (5 μM, in 50 mM Tris, pH 7.4, 5 mM GSH) at varying incubation times with 1 eq (solid triangles) and 20 eq (hollow triangles) of Cu^+. Signals from enzymatic reaction with luciferase are integrated over 1 h, following incubation with Cu^+ and expressed relative to the signal at 0 min incubation time.

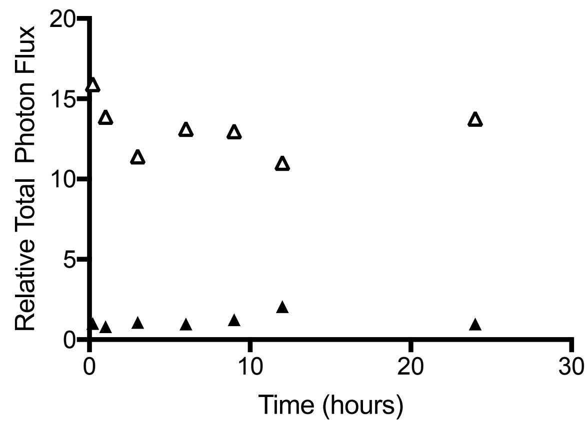

FIGURE S2. Stability of CCL-1 in serum-containing media (5 μM in DMEM containing 10% FBS, 5mM GSH as a reducing agent) in the presence (hollow triangles) or absence (solid triangles) of Cu^{+} (100 μM, 20 eq) over a 24-hour period. Signals from enzymatic reaction with luciferase are integrated over 1 h following the designated incubation times in the media, and expressed relative to the signal with no copper at 0 min incubation time.

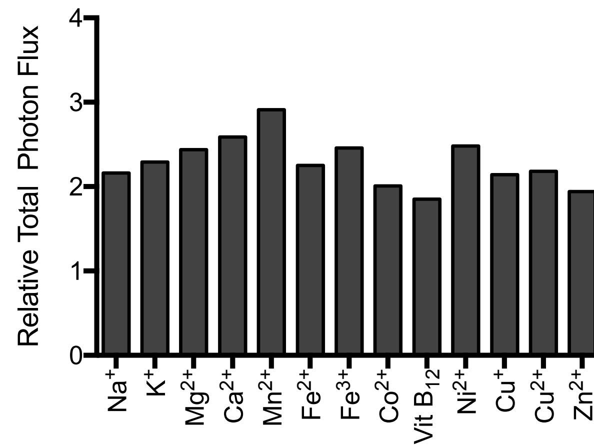

FIGURE S3. Relative bioluminescence response of D-luciferin (100 nM, in 50 mM Tris, pH 7.4, 5 mM GSH) after 1 h incubation with various biologically relevant s-block (1mM) and d-block (100 μM) metal ions and cobalamin (Vitamin B_{12}). Signals are integrated over 1 h and expressed as relative photon fluxes normalized to D-luciferin bioluminescence with no metal ion treatment.

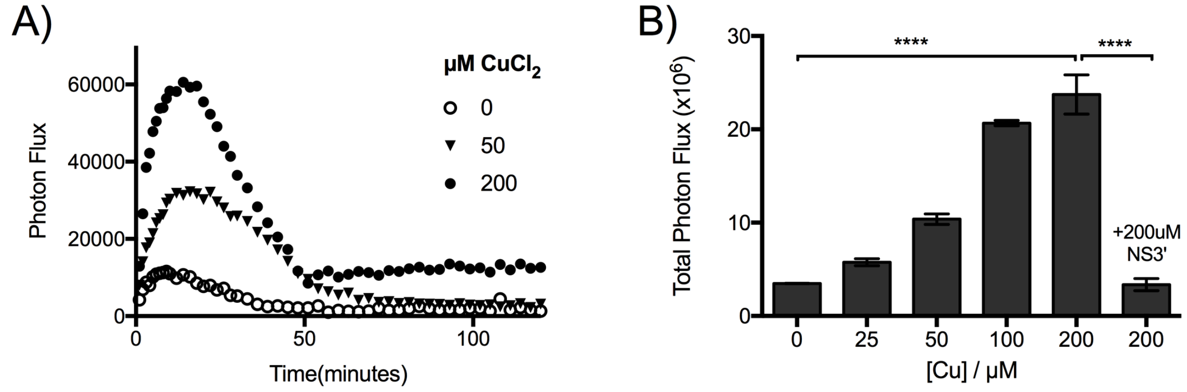

FIGURE S4. (A) Time-dependent bioluminescent signal generation of CCL-1 in PC3-Luc cells. (B) Bioluminescent signals from LNCaP-Luc cells. Cells were supplemented with $CuCl_2$ for 24 h, followed by addition of CCL-1 (25 μM) ± the copper chelator NS3' (200 μM). Total photon flux was integrated over 2 h. Statistical analyses were performed with a two-tailed Student's test. ****P ≤ 0.0001, and error bars are ±SD (n = 3).

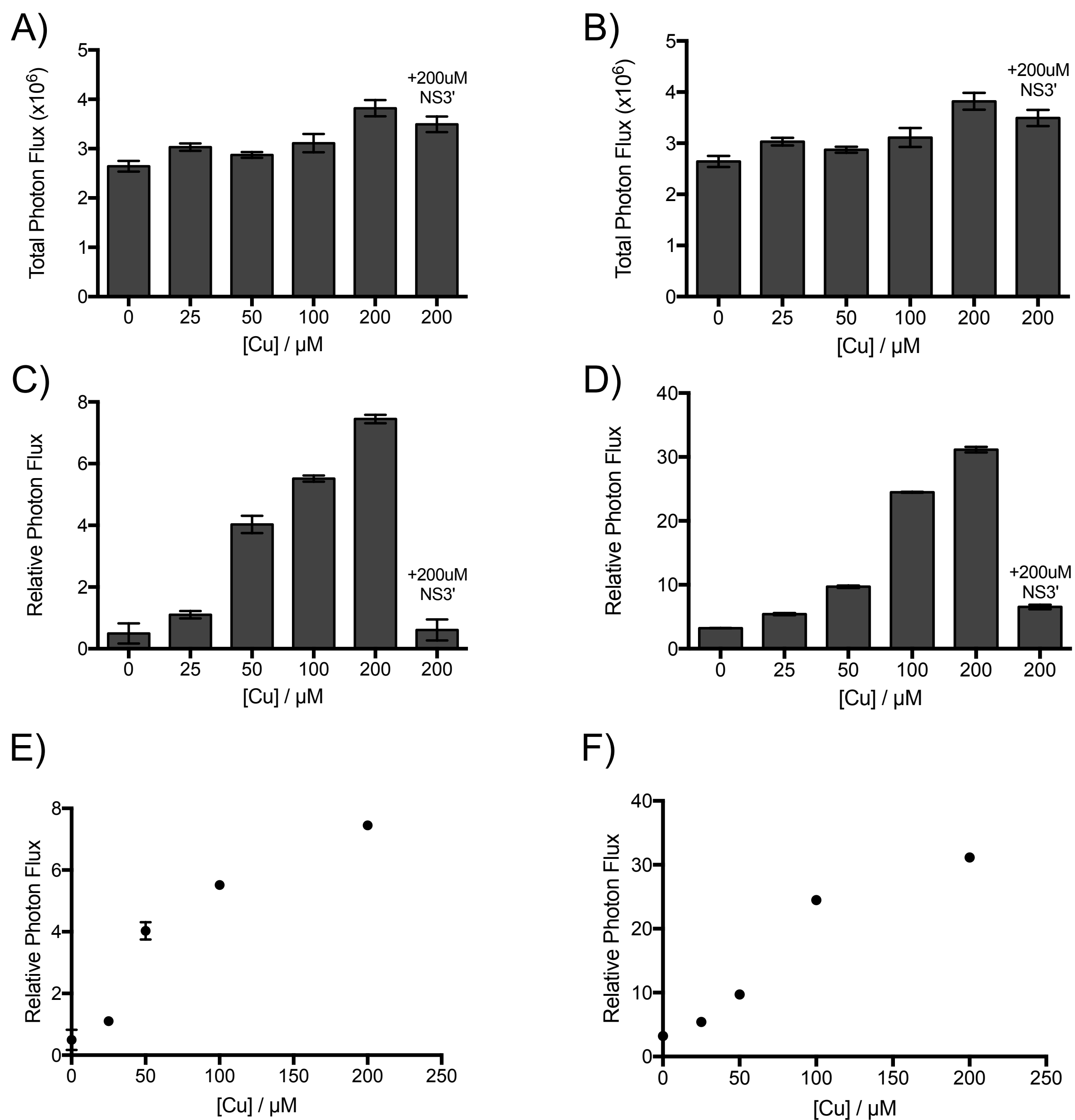

FIGURE S5. Panel A and B: Bioluminescent signals from (A) PC3-Luc cells and (B) LNCaP-Luc cells supplemented with $CuCl_2$ for 24 h, followed by addition of D-luciferin (1 µM) ± the copper chelator NS3' (200 µM). Total photon flux was integrated over 2 h. Error bars are ±SD (n = 4). Panel C and D: Bioluminescent signals of CCL-1 normalized to D-luciferin signals from (C) PC3-Luc cells and (D) LNCaP-Luc cells treated under the same conditions (supplemented with $CuCl_2$ for 24 h, followed by addition probe and ± the copper chelator 200 µM copper chelator NS3'). Total photon flux was integrated over 2 h. Error bars are ±SD (n = 4). Panel E and F: Dose-response curves for copper treatment with CCL-1 imaging in (E) PC3-Luc and (F) LNCaP-Luc cells were generated from the data shown in panels C and D.

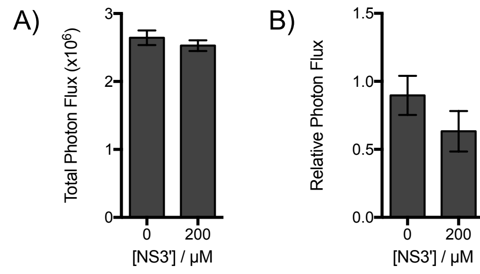

FIGURE S6. (A) Bioluminescent signals from PC3M-luc cells ± NS3' (200 μM) and imaged with D-luciferin (1 μM). Total photon flux was integrated over 2 h. Error bars are ± SD (n = 4). (B) Bioluminescent signals from PC3M-luc cells ± NS3' (200 μM) imaged with CCL-1 and normalized to the signal from cells imaged with D-luciferin under the same treatment conditions (Panel A).

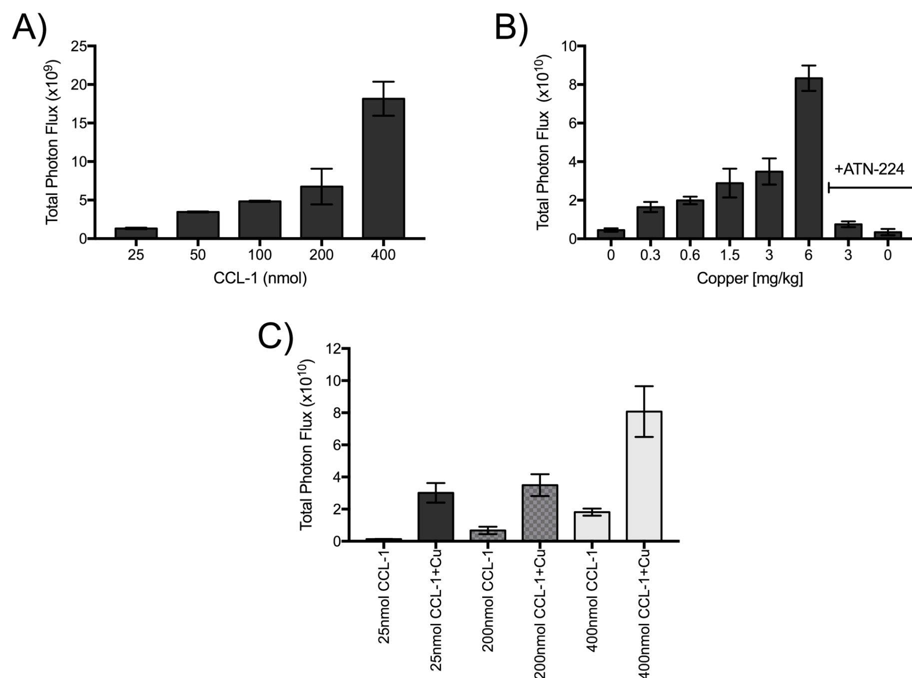

FIGURE S7. (A) Basal levels of copper can be detected in FVB-luc$^+$ with a CCL-1 dose-dependence. Mice were injected with 25 nmol, 50 nmol, 0.1 µmol, 0.2 µmol, and 0.4 µmol CCL-1 and total photon flux was acquired 0-60 min post-injection; n = 3-5 and error bars are ± SEM. (B) Mice pretreated with varying amounts of $CuCl_2$ and imaged with CCL-1 exhibit increasing bioluminescent signal as a function of copper concentration. FVB-luc$^+$ mice were injected (i.p.) with CCL-1 (0.2 µmol) after i.p. injection of vehicle, varying amounts $CuCl_2$, and/or ATN-224 (5 mg/kg). Injection of $CuCl_2$ and ATN-224 were performed 2 h and 10 min prior to injection CCL-1, respectively. Total photon flux was acquired 0-60 min post-injection; n ≥ 3 and error bars are ± SEM. (B) Mice pretreated with the same amount of $CuCl_2$ and imaged with varying doses of CCL-1 exhibit increases in bioluminescent signal relative to pretreatment with vehicle. FVB-luc$^+$ mice were injected (i.p.) with varying CCL-1 doses (25 nmol, 0.2 µmol, and 0.4 µmol) 2 hours after i.p. injection of vehicle or $CuCl_2$ (3 mg/kg). Total photon flux was acquired 0-60 min post-injection; n ≥ 4 and error bars are ± SEM.

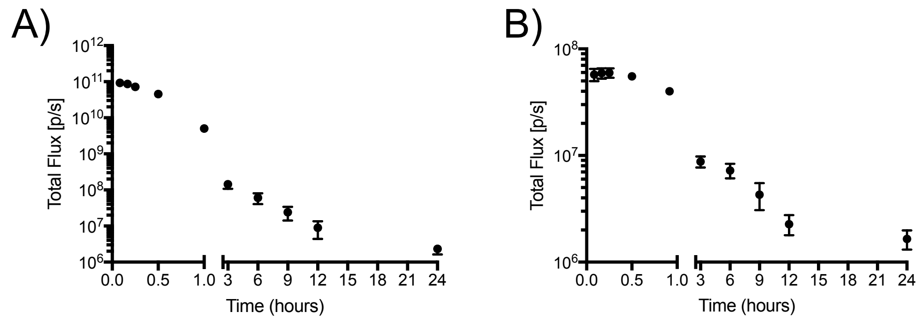

FIGURE S8. Metabolic clearance of bioluminescent probe in FVB-luc$^+$ mice injected with (A) 0.2 µmol D-luciferin or (B) 0.2 µmol CCL-1 in a 24-hour time period after probe injection. n = 3 and 4, respectively and error bars are ± SEM.

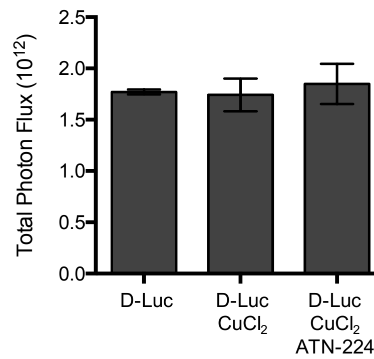

FIGURE S9. Bioluminescence imaging of FVB-Luc$^+$ mice with D-luciferin shows no change in signal with copper status. Total photon flux, 0-30 min post-injection, of FVB-Luc$^+$ mice injected (i.p.) with D-luciferin (D-Luc, 0.2 μmol) after i.p. injection of vehicle, $CuCl_2$ (3 mg/kg), or both $CuCl_2$ (3 mg/kg) and ATN-224 (5 mg/kg). Injection of $CuCl_2$ and ATN-224 were performed 2 h and 10 min prior to injection D-luciferin, respectively. Values are reported with error bars as ±SEM (n = 3-5).

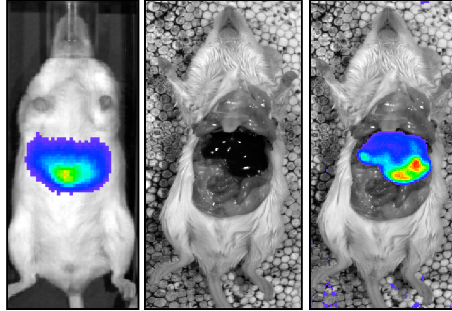

FIGURE S10. Imaging of CCL-1 in liver-specific luciferase-expressing mice, with bioluminescence signal generated specifically in the liver. Images were acquired in the intact organism (left) and after opening the peritoneal cavity for organ visualization by white light (middle) and bioluminescence (right).

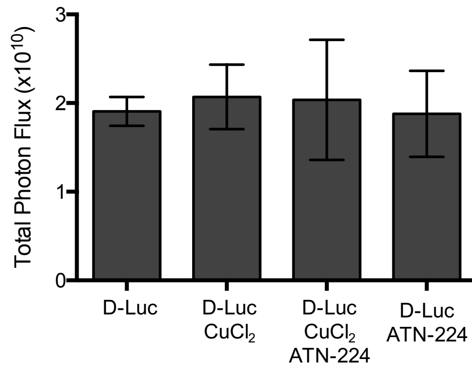

FIGURE S11. Bioluminescence imaging of liver-specific luciferase-expressing (L-Luc) mice with D-luciferin shows no change in signal with copper status. Total photon flux, 0-30 min post-injection, of L-Luc mice injected (i.p.) with D-luciferin (D-Luc, 0.1 μmol) after i.p. injection of vehicle, $CuCl_2$ (3 mg/kg) alone, both $CuCl_2$ (3 mg/kg) and ATN-224 (5 mg/kg), or ATN-224 (30 mg/kg) alone. Injections of $CuCl_2$ or ATN-224 alone were performed 2 h prior to injection of D-Luciferin. Mice injected with both $CuCl_2$ and ATN-224 were injected 2h and 10 min prior to injection of D-Luciferin, respectively. Values are reported with error bars as ±SEM (n = 3-5).

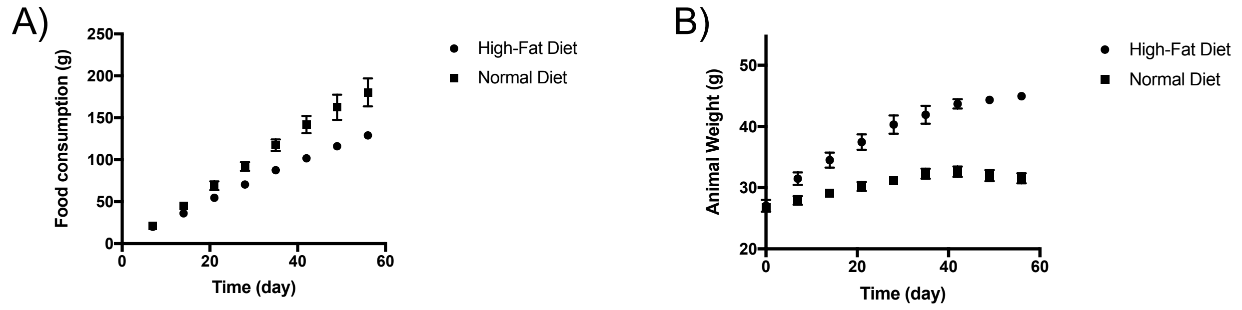

FIGURE S12. Monitoring animal food consumption and weight gain in a diet-induced model of NAFLD with L-luc mice. (A) Food consumption of each cage of 3-5 mice was monitored weekly for mice on the high-fat diet and mice fed normal chow. Data are represented as average food consumption per mouse. Error bars are ±SEM (n = 6). (b) Animal weights were monitored weekly for the two groups. Error bars are ±SEM (n = 6).

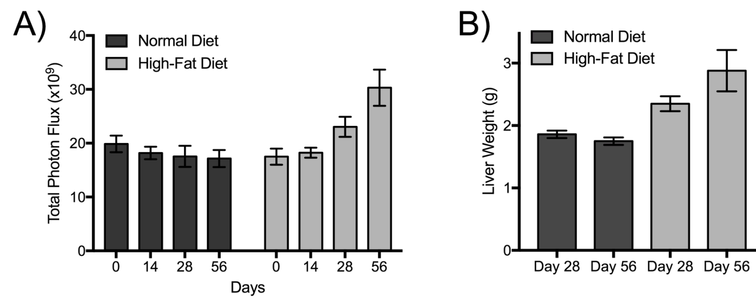

FIGURE S13. Bioluminescent signal from imaging L-Luc mice with D-luciferin increases with liver size in mice fed high-fat diets. (A) Bioluminescent signal from D-luciferin of L-Luc mice placed on high-fat diet or normal feeding conditions. Data is represented as integrated photon flux over 30 min. Error bars are ± SEM (n ≥ 9) (B) Weights of the livers of L-Luc mice sacrificed 28 and 56 days after feeding on high-fat or normal diets. Error bars are ± SEM (n ≥ 4)

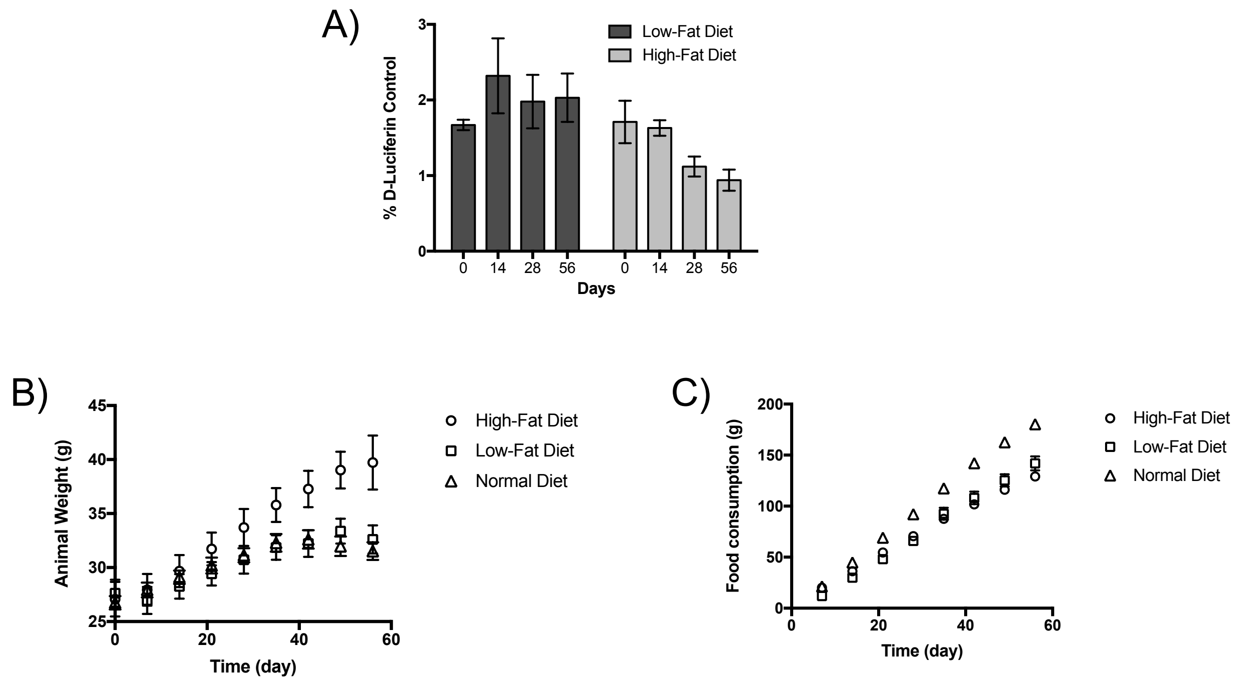

FIGURE S14. Bioluminescence imaging, animal food consumption, and weight gain in a diet-induced model of NAFLD with L-luc mice as compared to L-luc mice fed a low-fat diet with equivalent copper content. In this study, mice from the same two litters were divided into two groups per litter and fed either high-fat diets or low-fat diets. (A) Bioluminescent signal from CCL-1 (normalized to D-luciferin) of L-Luc mice placed on a high-fat diet or low-fat diet. Mice were imaged at week 0, 2, 4, and 8 after i.p. injection of D-luciferin followed by CCL-1 2 days later. Error bars are ± SEM (n ≥ 4). (B) Food consumption of each cage of 2-5 mice was monitored weekly for mice on the high-fat diet and mice fed normal chow. Data are represented as average food consumption per mouse. Error bars are ±SEM (n ≥ 4). (b) Animal weights were monitored weekly for the two groups. Error bars are ±SEM (n ≥ 4).

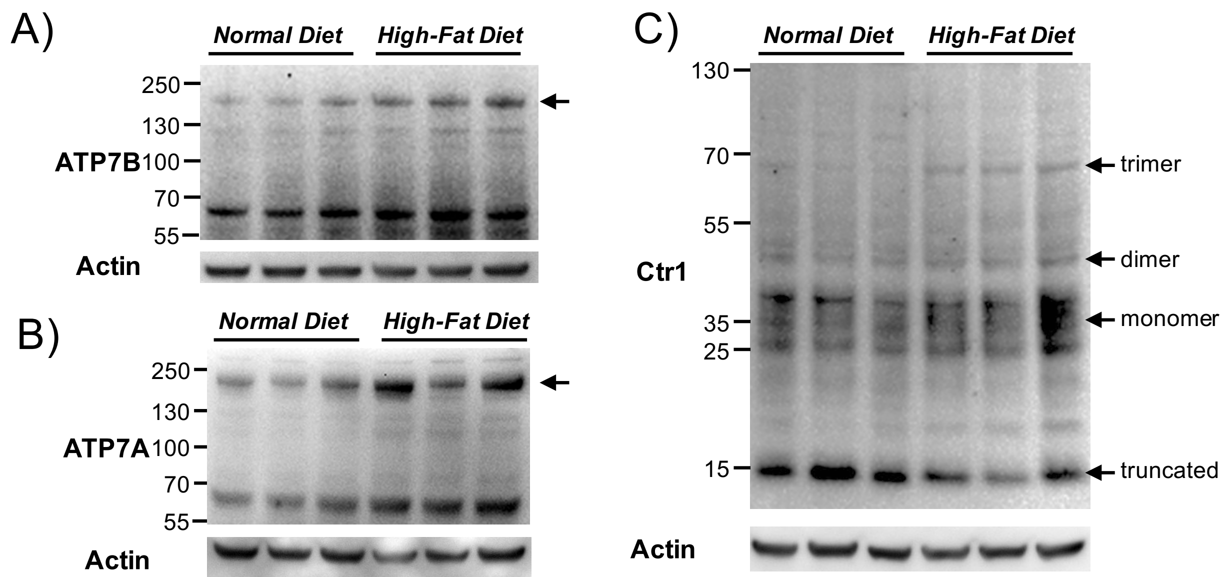

FIGURE S15. SDS-PAGE analysis of liver extracts of three mice fed normal diets and three HFD mice. Expanded Western blots for (A) ATP7B, (B) ATP7A, and (C) Ctr1. Arrows indicate the proteins of interest and actin blots were used as loading controls.